Capacitive and Solution Resistance Effects on Voltammetric Responses at a Disk Microelectrode Covered with a Self-Assembled Monolayer in the Presence of Electron Hopping

ARTICLE *in* ANALYTICAL CHEMISTRY · SEPTEMBER 2009

Impact Factor: 5.64 · DOI: 10.1021/ac901513x · Source: PubMed

4 AUTHORS, INCLUDING:

Oleksiy V Klymenko
Imperial College London
72 PUBLICATIONS **1,338** CITATIONS
SEE PROFILE

Irina Svir
Ecole Normale Supérieure de Paris
82 PUBLICATIONS **834** CITATIONS
SEE PROFILE

Anal. Chem. **2009,** *81,* 8545–8556

Capacitive and Solution Resistance Effects on Voltammetric Responses at a Disk Microelectrode Covered with a Self-Assembled Monolayer in the Presence of Electron Hopping

Christian Amatore,*,† Alexander Oleinick,†,‡ Oleksiy V. Klymenko,‡ and Irina Svir*,†,‡

Département de Chimie, Ecole Normale Supérieure, UMR CNRS-ENS-UPMC 8640 "PASTEUR", 24 rue Lhomond, 75231 Paris Cedex 05, France, and Mathematical and Computer Modelling Laboratory, Kharkov National University of Radioelectronics, 14 Lenin Avenue, 61166 Kharkov, Ukraine

This article extends our previous works (Amatore, C.; Oleinick, A.; Svir, I. *Anal. Chem.* 2008, *80,* 7947–7956; 7957–7963.) about the effects of resistive and capacitive distortions in voltammetry at disk microelectrodes. The particular case of voltammetry of a self-assembled monolayer carrying one redox site per molecule is investigated here. In addition, the effect of an uneven distribution of the effective electrochemical potential on the possibility of electron hopping (EH) contributions is examined. An original model of EH has been developed considering both diffusion-type (i.e., related to concentration gradients) and migration-type (i.e., imposed by an uneven distribution of the electrical potential due to an ohmic drop and capacitance charging) contributions. This predicts that as soon as the system performs out of thermodynamic equilibrium and provided that the EH rate constants are not too small the system tends to re-establish its out-of-equilibrium state through EH. Hence, EH somewhat tries to compensate the voltammetric distortions that would be enforced by the uneven distribution of the electrochemical driving force incurred by the system due to an ohmic drop and capacitive charging. However, this rigorous analysis established that, though EH may be effective under specific circumstances particularly near the electrode edge, its overall influence on voltammetric waves remains negligible for any realistic experimental situation.

In this work we consider a self-assembled monolayer (SAM) formed of an electroactive species A tethered to a disk microelectrode surface of radius r_d by an inert bridge and with a surface concentration Γ^0 (Figure 1). We assume that the redox commutation of the electroactive headgroup

$$A^z + ne \underset{k_b}{\overset{k_f}{\rightleftharpoons}} B^{z-n} \qquad (1)$$

occurs under potential control at the electrode surface, where k_f and k_b are the forward and backward rate constants of the heterogeneous electron transfers (ETs), respectively. These rate constants are supposed to be potential-dependent and to obey a generalized Butler−Volmer expression:[1]

$$k_{f,b} = k_0 \exp\left[\begin{matrix}-\alpha \\ (1-\alpha)\end{matrix} \frac{nF}{R_g T} E^*\right] \qquad (2)$$

where k_0 is the standard electrochemical rate constant, α is the transfer coefficient, F is the Faraday constant, R_g is the gas constant, T is the temperature, and E^* is the local potential applying to the site of electron transfer.

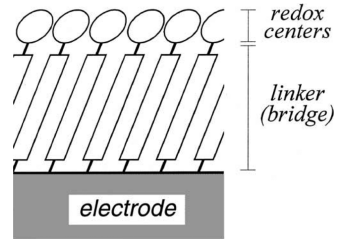

Figure 1. Scheme of a monolayer covering a disk microelectrode.

In the present work we examine the possible distortions due to lateral electron hopping driven by the uneven ohmic drop and capacitive charging of the system,[2] hence the uneven distribution of kinetics of direct faradic reactions across the disk surface. Indeed, E^* is related to the potential $E(t)$ applied to the disk metallic conductor by[2]

$$E^*(r,t) = E(t) - E^0 - \mathrm{d}i(r,t)\,\mathrm{d}R_e(r) \qquad (3)$$

where $E = E_{in} + vt$ with E_{in} the initial potential and v the algebraic value of the voltammetric scan rate, E^0 is the formal potential of the A/B redox couple, and $\mathrm{d}i(r,t)\,\mathrm{d}R_e(r)$ is the ohmic drop applying at the electrode point at a distance r from its center. In eq 3, $\mathrm{d}i(r)$ is the overall (capacitive + faradic) current flowing toward the bulk electrolyte solution (i.e., above the SAM surface) in the form of an ionic flux through the infinitesimal ring with radius r and thickness $\mathrm{d}r$, while $\mathrm{d}R_e(r)$ is

* Corresponding authors. E-mail: christian.amatore@ens.fr (C.A.); irina.svir@kture.kharkov.ua, irina.svir@ens.fr (I.S.). Fax: +33-1-4432-3863.
† UMR CNRS-ENS-UPMC 8640 "PASTEUR".
‡ Kharkov National University of Radioelectronics.

(1) Bard, A. J.; Faulkner, L. R. *Electrochemical Methods: Fundamentals and Applications*; Wiley & Sons: New York, 2001.
(2) Amatore, C.; Oleinick, A.; Svir, I. *Anal. Chem.* **2008**, *80*, 7947–7956.

10.1021/ac901513x CCC: $40.75 © 2009 American Chemical Society
Published on Web 09/17/2009

the uncompensated resistance of the current tube limited by the same ring on the SAM surface.[2] Note that though both $di(r,t)$ and $dR_e(r)$ are differential elements their product has a finite value owing to the fact that currents scale with the surface element area while resistance is reciprocal with the surface element area. Because of the dependence upon the cylindrical symmetry of each of these factors (i.e., current and resistance), it is more adequate to consider them as relative to the series of infinitesimally small rings of radius r and thickness dr which describe the system surface. This does not affect the value of $di(r,t)\ dR_e(r)$ at each electrode point since each point within such an elementary ring is submitted to the same ohmic drop. Hence, this value depends only on the distance of a particular point or ring from the center of the electrode (see ref 2 and below).

In previous works[2,3] we established that, due to ohmic drop and capacitive charging of the system, the effective potential E^* governing the rate laws in eq 2 is distributed unevenly across the electrode surface and may be significantly different from the applied potential E. As a result, whenever the relative surface concentrations of the A and B headgroups are controlled by kinetics (viz., by the local value of E^* and its effect on kinetic rate constants) rather than by thermodynamics, the electrochemical potential of the redox headgroups may become anisotropic so that a trend to re-establish the out-of-equilibrium situation will occur by electron hopping.

When the rate constants in eq 2 are fast compared to the scan rate, adequate electron exchanges with the underlying electrode surface are expected to achieve equilibrium of the redox headgroups at each particular value of E^* at each instant. However, when this is not the case, the heterogeneous rate constants cannot restore any out-of-equilibrium situation that may occur across the SAM surface.

Hence, the anisotropy of the electrochemical potential across the SAM surface will enforce lateral cross-talk between adjacent redox centers within the SAM (electron hopping). Note that the rate at which electron hopping may restore the out-of-equilibrium situation depends also on the time scale owing to the values of the corresponding 2D bimolecular rate constants. Hence, this phenomenon will also be limited ultimately when involving the ultrafast voltammetric scans required to measure the kinetics of electron exchange across the SAM molecular bridges.[4]

However, the two types of kinetics are different, so there is a priori no reason for the two kinetic processes (i.e., unimolecular and heterogeneous between the electrode and one headgroup across the molecular bridge, or bimolecular and 2D homogeneous between adjacent headgroups in the SAM) to be in phase. This remark prompted us to investigate with particular emphasis the possible role of EH in conjunction with ohmic and capacitive alterations in the voltammetry of SAM systems so as to examine whether the fact that EH is usually not considered may lead to appreciable errors in rationalizing voltammetric data pertaining to such systems.

Note that, since we thoroughly investigated and reported the effects of uneven ohmic and capacitive phenomena across a disk surface in 2D redox systems, the readers are referred to our previous work in ref 2 for these detailed analyses. However, since it will be shown hereafter that lateral EH may exist only when the system is in out-of-redox equilibrium, but is then controlled by ohmic and capacitive distortions, the present theoretical evaluation of EH requires these factors to be incorporated into the following theoretical analysis.

THEORY

EH with a Migration Contribution in SAMs. In classical formulations of EH[5] one generally considers that the only driving force sustaining EH stems from the local concentration gradients. In the present case we need to consider that two gradients (concentration and effective potential E_{SAM} experienced by the SAM molecules) exist simultaneously due to the uneven distribution of the electrical potential across the SAM and both contribute to the electrochemical potential's anisotropy across the SAM surface:

$$\mu_A = \mu_A^0 + R_gT \ln \Gamma_A + zFE_{SAM} \quad (4)$$

$$\mu_B = \mu_B^0 + R_gT \ln \Gamma_B + (z - n)FE_{SAM} \quad (5)$$

where μ_m and μ_m^0 are, respectively, the electrochemical potential of species m = A, B and their standard value[1] while E_{SAM} is the local electrical potential.

The potential E_{SAM} experienced by the redox centers of adsorbed molecules may be expressed through the following relation obtained by rearranging eq 3:

$$E_{SAM}(r,t) = E^0 + di(r,t)\ dR_e(r) = E(t) - E^*(r,t) \quad (6)$$

The physical meaning of E_{SAM} is readily apparent from the consideration of Figure 2. Thus, the potential applied to the electrode is a sum of two effective potentials:

$$E(t) = E^*(r,t) + E_{SAM}(r,t) \quad (7)$$

where E^* controls electron transfers between redox centers and the electrode while E_{SAM} reflects the fact that these redox centers probe a potential different from that prevailing at infinity due to the local ohmic drop. Since $di(r,t)\ dR_e(r)$ is expected to vary across the SAM, both E_{SAM} and $E^*(r,t)$ are likely to vary.

Hence, to evaluate the role of electron hopping in relaxing the system anisotropy, we need first to elaborate a specific model of EH which encompasses the two sources of anisotropy. For this purpose we will develop a semimicroscopic analysis of the 2D system at hand following the principles of previous approaches developed for modeling pure diffusional EH[5] though that will be expanded to account for work terms (compare eqs 4 and 5).

(3) Amatore, C.; Oleinick, A.; Svir, I. *Anal. Chem.* **2008**, *80*, 7957–7963.
(4) Amatore, C.; Maisonhaute, E.; Schöllhorn, B.; Wadhawan, J. *ChemPhysChem* **2007**, *8*, 1321–1329.

(5) (a) Murray, R. W. *Philos. Trans. R. Soc. London, A* **1981**, *302*, 253. (b) Dahms, H. J. *J. Phys. Chem.* **1968**, *72*, 362. (c) Ruff, I.; Friedrich, V. J. *J. Phys. Chem.* **1971**, *75*, 3297. (d) Ruff, I.; Friedrich, V. J.; Demeter, K.; Csillag, K. *J. Phys. Chem.* **1971**, *75*, 3303. (e) Andrieux, C. P.; Savéant, J. M. *J. Electroanal. Chem.* **1980**, *111*, 377. (f) Laviron, E. *J. Electroanal. Chem.* **1980**, *112*, 1. (g) Blauch, D. N.; Savéant, J. M. *J. Am. Chem. Soc.* **1992**, *114*, 3323. (h) Blauch, D. N.; Savéant, J. M. *J. Phys. Chem.* **1993**, *97*, 6444. (i) Gorman, C. *Adv. Mater.* **1998**, *10*, 295. (j) Tomalia, D. A.; Naylor, A. M.; Goddard, W.A., III. *Angew. Chem., Int. Ed. Engl.* **1990**, *29*, 138. (k) For reviews see, e.g.: Murray, R. W. *Molecular Design of Electrode Surfaces*; Wiley & Sons: New York, 1992.

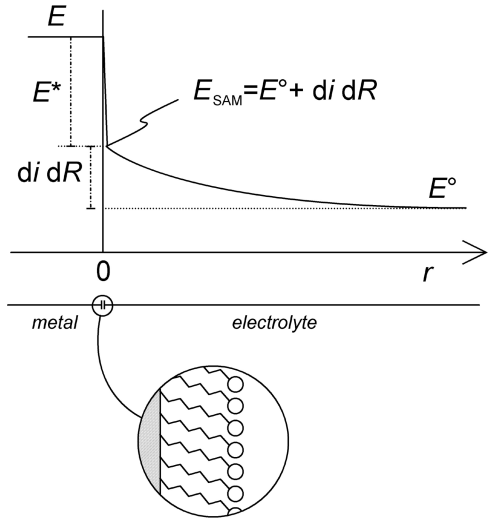

Figure 2. Scheme of the effective potentials $E^*(r,t)$ and $E_{SAM}(r,t)$. Note that for the sake of simplification we assigned the value at infinite distance as equal to E^0; this introduces just a vertical off-scale factor, the exact value of which is irrelevant here.

Let us consider a closed circular frontier between two elementary rings of thickness dr located on each side of the circle of radius r (d$r \le r \le r_d -$ dr) and possible electron transfer occurring during the elementary time interval dt between the couples A/B located within each ring. The corresponding EH processes are driven simultaneously by the local concentration gradients (i.e., diffusion-like) and by those of E_{SAM} since this acts on the local stability of charges (i.e., migration-like) and is also reflected in the electrochemical potential (eqs 4 and 5). Both variables (i.e., local concentrations and local E_{SAM} values) are modulated by faradic reactions with the underlying electrode and are in turn modulated by the E^* distribution across the disk. When the system is not at thermodynamic equilibrium or when a radial gradient of E^* (hence that of $-E_{SAM}$; see eq 7 and Figure 2) exists across the SAM, the above convoluted process tends to spontaneously provoke a redistribution of redox centers across the SAM. This redistribution involves no net exchange of charges with the metal electrode, so it does not correspond to any additional faradic current contribution over the whole electrode surface. However, it corresponds to a discrepancy between the local faradic current delivered by the metal and that carried into the solution from this point of the SAM by ionic movements. Hence, when this EH redistribution of charges occurs, it affects the local ohmic drop and, as a consequence, the charging current contribution. This interplay among all variables creates a complex convoluted situation as soon as the system is not at thermodynamic equilibrium or experiences a radial gradient of E^*. It is the purpose of the following to examine in full detail this convoluted process, which requires in particular the treatment of EH under the conditions where a migration contribution acts.

EH provokes an apparent displacement of dN_A molecules of A across the boundary of length $2\pi r$ from the inner to the outer elementary ring, hence an apparent flux $J^{EH}_{A,r}(r)$

$$J^{EH}_{A,r} = \left(\frac{dN_A}{2\pi r\, dt}\right)^{EH} \quad (8)$$

due to the opposite displacement of nF dN_A electrons which gives rise to a local radial faradic current moving across the SAM though its overall effect over the SAM involves no net exchange of charge:

$$i^{EH} = nF\left(\frac{dN_A}{dt}\right)^{EH} = nF(2\pi r)J^{EH}_{A,r} \quad (9)$$

To evaluate the value of $J^{EH}_{A,r}(r)$, we remark that at the microscopic level this flux corresponds to a variation of the surface concentration $\Gamma_A(r)$ regulated by local EH rate constants which in turn are modulated by the gradient of E_{SAM} (note that, in the absence of any gradient of E_{SAM}, $k^+ = k^-$ as is usually considered in developing EH models[5]):

$$[d\Gamma(r)]^{EH} = \left(\frac{dN_A}{2\pi r\, dr}\right)^{EH} = \left[k^+\Gamma_A\left(r - \frac{dr}{2}\right)\Gamma_B\left(r + \frac{dr}{2}\right) - k^-\Gamma_A\left(r + \frac{dr}{2}\right)\Gamma_B\left(r - \frac{dr}{2}\right)\right] dt \quad (10)$$

where $r \pm$ dr/2 corresponds to the middle of each elementary ring concerned.

When there is no change of energy associated with the electron hopping steps, the two 2D bimolecular EH rate constants are equal, $k^+ = k^- = k_0^{EH}$, where k_0^{EH} is the intrinsic 2D electron transfer rate constant.[5] However, when EH occurs between two regions with different electrical potentials, k^+ and k^- necessarily differ because each rate constant must take into account the energetic change d$W^\pm$ associated with each electron transfer across the boundary. Indeed, according to classical kinetic theories, one has

$$k^\pm = k_0^{EH} e^{-\beta(dW^\pm/R_gT)} \quad (11)$$

where k_0^{EH} is the intrinsic EH rate constant (viz., at d$W^\pm = 0$) and β a Brönsted coefficient (transfer coefficient). This is close to 1/2 since d$W^\pm$ values are expected to be small for adjacent molecules and the system to be very close to full symmetry during each electron hopping step.[6]

With the signs used in eq 8, k^+ corresponds to A (charge z) apparently moving across the circular boundary at r from the inner ring where it probed the electrical potential $E_{SAM}(r -$ d$r/2)$ to the outer one where $E_{SAM}(r +$ d$r/2)$ prevails; simultaneously B (charge $z - n$) apparently experiences the opposite change, i.e., from $E_{SAM}(r +$ d$r/2)$ to $E_{SAM}(r -$ d$r/2)$.

Hence, the electrical work term contribution to the activation barrier controlling k^+ is

$$\begin{aligned} dW^+ &= zF[E_{SAM}(r + dr/2) - E_{SAM}(r - dr/2)] + \\ &\quad (z - n)F[E_{SAM}(r - dr/2) - E_{SAM}(r + dr/2)] = \\ &\quad nF[E_{SAM}(r + dr/2) - E_{SAM}(r - dr/2)] = \\ &\quad nF(\text{grad}\, E_{SAM})\, dr = -nF(\text{grad}\, E^*)\, dr \end{aligned} \quad (12)$$

since grad $E_{SAM} = -$(grad E^*) (compare eq 7). For k^-, this becomes by symmetry

$$dW^- = nF(\text{grad}\, E^*)\, dr \quad (13)$$

Note that here we consider only energetic changes due to the electrical potential gradient, but the same formalism would apply

to any other energy gradient, the term grad(nFE^*), which considers only electrical work terms, then being replaced by the gradient of the corresponding sum of energies. Within this formalism, one then has

$$k^{\pm} = k_0^{EH} e^{-\beta(dW^{\pm}/R_gT)} \approx k_0^{EH}\left(1 - \beta\frac{dW^{\pm}}{R_gT}\right) = k_0^{EH}\left(1 \pm \beta\frac{nF}{R_gT}(\text{grad } E^*)\, dr\right) \quad (14)$$

One can then rewrite the surface flux due to EH as

$$J_{A,r}^{EH} = \frac{dN_A}{2\pi r\, dt} = [k^+\Gamma_A^-(\Gamma^0 - \Gamma_A^+) - k^-\Gamma_A^+(\Gamma^0 - \Gamma_A^-)]\, dr = [(k^- - k^+)\Gamma_A^-\Gamma_A^+ + \Gamma^0(k^+\Gamma_A^- - k^-\Gamma_A^+)]\, dr \quad (15)$$

where we note for simplification that $\Gamma_A^+ = \Gamma_A(r + dr/2)$, $\Gamma_A^- = \Gamma_A(r - dr/2)$, and $\Gamma_A = \Gamma_A(r)$. Remarking that $\Gamma_A^- = \Gamma_A(r) - (\text{grad } \Gamma_A)(dr/2)$ and $\Gamma_A^+ = \Gamma_A(r) + (\text{grad } \Gamma_A)(dr/2)$ and developing to the first order in dr, we obtain

$$\Gamma_A^-\Gamma_A^+ \cong [\Gamma_A(r)]^2 + \Gamma_A(r)\left[(\text{grad } \Gamma_A)\frac{dr}{2} - (\text{grad } \Gamma_A)\frac{dr}{2}\right] = [\Gamma_A(r)]^2 \quad (16)$$

that is

$$(k^- - k^+)\Gamma_A^-\Gamma_A^+ \cong -k_0^{EH} 2\beta\frac{nF}{R_gT}(\text{grad } E^*)[\Gamma_A(r)]^2\, dr \quad (17)$$

On the other hand, one has

$$k^+\Gamma_A^- = k_0^{EH}\left[1 + \beta\frac{nF}{R_gT}(\text{grad } E^*)\, dr\right]\left[\Gamma_A(r) - (\text{grad } \Gamma_A)\frac{dr}{2}\right] \cong k_0^{EH}\left[\Gamma_A - (\text{grad } \Gamma_A)\frac{dr}{2} + \Gamma_A\beta\frac{nF}{R_gT}(\text{grad } E^*)\, dr\right] \quad (18)$$

and

$$k^-\Gamma_A^+ = k_0^{EH}\left[1 - \beta\frac{nF}{R_gT}(\text{grad } E^*)\, dr\right]\left[\Gamma_A(r) + (\text{grad } \Gamma_A)\frac{dr}{2}\right] \cong k_0^{EH}\left[\Gamma_A + (\text{grad } \Gamma_A)\frac{dr}{2} - \Gamma_A\beta\frac{nF}{R_gT}(\text{grad } E^*)\, dr\right] \quad (19)$$

where again the two series developments are limited to the first order in dr. Therefore

$$J_A^{EH}(r) = k_0^{EH}\Gamma^0(dr)^2\left[-(\text{grad } \Gamma_A) + 2\beta\frac{nF}{R_gT}(\text{grad } E^*)\Gamma_A - 2\beta\frac{nF}{R_gT}(\text{grad } E^*)\frac{\Gamma_A^2}{\Gamma^0}\right] \quad (20)$$

Let us remark that the dimension of k_0^{EH} is mol^{-1} [L]^2 [T]$^{-1}$ (where [L] denotes a unit of length and [T] a unit of time), that of Γ_A is mol [L]$^{-2}$, and that of dr is [L]; therefore, the dimension of $k_0^{EH}\Gamma^0(dr)^2$ is [L]^2 [T]$^{-1}$, which is equal to that of a diffusion coefficient. For this reason and as usual in electron hopping models,[5] we note that

$$D^{EH} = k_0^{EH}\Gamma^0(dr)^2 \quad (21)$$

Note that in fact we obtain here the classical formulation of the EH diffusion coefficient[5] since at the microscopic level dr represents the distance between two adjacent sites along one radial coordinate. Equation 18 is then reformulated as follows:

$$J_A^{EH} = -D^{EH}\left[(\text{grad } \Gamma_A) - 2\beta\frac{nF}{R_gT}\Gamma_A(\text{grad } E^*)\left(1 - \frac{\Gamma_A}{\Gamma^0}\right)\right] \quad (22)$$

On one hand, this expression allows expressing the radial faradic current in eq 9. Hence, by application of the Kirchhoff circuit node law to an elementary ring of radius r and thickness dr, the fraction of the faradic current exchanged with the underlying electrode which is finally transferred toward the solution, giving rise to the local ionic current developing from this ring element, is

$$di_f = -nF(2\pi r)\left\{D^{EH}\left[(\text{grad } \Gamma_A) - 2\beta\frac{nF}{R_gT}\Gamma_A(\text{grad } E^*) \times \left(1 - \frac{\Gamma_A}{\Gamma^0}\right)\right] + [k_f\Gamma_A - k_b(\Gamma^0 - \Gamma_A)]\, dr\right\} \quad (23)$$

though in the following we prefer to formulate it by remarking that it is proportional to the time gradient of the local surface concentration of A (see below, eq 27).

On the other hand, through application of the second Fick law, eq 22 affords the rate law governing the time variation of $\Gamma_A(r)$ due to the EH process. One obtains

$$\left(\frac{\partial\Gamma_A}{\partial t}\right)_r^{EH} = -(\text{div } J_A^{EH}) = \text{div}\left\{D^{EH}\left[(\text{grad } \Gamma_A) - 2\beta\frac{nF}{R_gT}\Gamma_A(\text{grad } E^*)\left(1 - \frac{\Gamma_A}{\Gamma^0}\right)\right]\right\} \quad (24)$$

i.e.

$$\left(\frac{\partial\Gamma_A}{\partial t}\right)_r^{EH} = D^{EH}\left\{\Delta\Gamma_A - 2\beta\frac{nF}{R_gT}\frac{1}{\Gamma^0}[\Gamma_A(\Gamma^0 - \Gamma_A)\Delta E^* + (\Gamma^0 - 2\Gamma_A)(\text{grad } \Gamma_A)(\text{grad } E^*)]\right\} \quad (25)$$

It is interesting to note that this equation has a structure similar to that of the Nernst−Plank−Fick equation since it includes both diffusion and migration terms while the usual EH equations involve only a diffusionnal term.[5] Note also that it differs from a previous law proposed by Savéant et al. which amounted to include a classical migration term in the classical electron hopping

diffusional law.[7] Equation 25 also differs from the Nernst−Plank equation in the sense that the migrational term (i.e., the bracketed term of eq 25) corresponds to electron transfers between immobile redox centers A and B rather than ionic displacements. This is reflected by the special structure of this term. Because of its bimolecular kinetic origin, it depends on the concentrations of both A and B. Interestingly, when the gradient of energy is absent, as is considered in usual electron hopping models,[5] the "migration" term disappears and the whole process appears as a pure diffusion, i.e., as a first-order process though it is fundamentally a second-order one. This confirms a posteriori our above claim that EH redistribution of surface concentrations is not playing any role when online electronic compensation of ohmic drop is performed during the voltammetric experiment.[4]

Finally, note also that eq 25 unifies elements that have been discussed separately in the electrochemistry of transport in polymeric films at electrodes.[8] Indeed, the term $D^{EH}\Delta\Gamma_A$ (viz., $D^{EH}\Delta C_A$ in a 3D case) represents the effect of the so-called concentration-independent diffusion coefficient, which reflects the free movement of redox carriers within the polymer network. Conversely, the terms in the brackets represent the effect of the so-called concentration-dependent diffusion coefficient which features movement by chemical or redox exchanges between sites of the matrix. This is readily apparent upon rewriting eq 25 as

$$\left(\frac{\partial\Gamma_A}{\partial t}\right)_r^{EH} = D^{EH}\Delta\Gamma_A - 2\beta\frac{D^{EH}}{\Gamma^0}\left\{\Gamma_A(\Gamma^0-\Gamma_A)\Delta\left(\frac{nFE^*}{R_gT}\right) + [(\Gamma^0-2\Gamma_A)(\text{grad}\,\Gamma_A)]\,\text{grad}\left(\frac{nFE^*}{R_gT}\right)\right\} \quad (26)$$

Furthermore, as stated above though we focused here on electrical potential when necessary the work term nFE^* may be replaced by any composite work term, for example, including other electrical and local specific chemical contributions, since the only point that matters in controlling the rate constants $k^{\pm}$ is the energetic change experienced by A and B during their apparent interchange.

Finally, considering in addition the role of electron exchanges with the subjacent metallic electrode through the molecular bridge, the total variation of Γ_A at r ($0 < r < r_d$) is given by

$$\left(\frac{\partial\Gamma_A}{\partial t}\right)_r = D^{EH}\left\{\Delta\Gamma_A - 2\beta\frac{nF}{R_gT}\frac{1}{\Gamma^0}[\Gamma_A(\Gamma^0-\Gamma_A)\Delta E^* + (\Gamma^0-2\Gamma_A)(\text{grad}\,\Gamma_A)(\text{grad}\,E^*)]\right\} - k_f\Gamma_A + k_b(\Gamma^0-\Gamma_A) \quad (27)$$

To conclude this section, we need to formulate the conditions applying at the center ($r = 0$) and edge ($r = r_d$) of the disk. At the center the gradient of Γ_A is necessarily zero because of symmetry, so that

$$\left(\frac{\partial\Gamma_A}{\partial r}\right)_0 = 0 \quad (28)$$

To evaluate the condition at the disk edge, we need first to remark that the radial currents that are generated at the SAM surface by EH simply redistribute the charges created within the whole SAM by the effective faradic currents exchanged between the redox headgroups and the electrode surface. Hence, globally they cannot feature a real macroscopic current flow between the electrode and the surrounding electrolyte solution. Conversely, they affect the local component of the current intensity which is flowing toward the solution from each point of the SAM surface. In other words, the overall faradic current flow has a single origin which is the series of individual electron transfer exchanges between the metallic electrode and each headgroup across its molecular bridge, and its overall effect cannot be changed following its redistribution across the SAM surface by EH.

Integration of eq 27 over the disk surface yields the overall faradic current through the electrode:

$$2\pi nF\int_0^{r_d}\left(\frac{\partial\Gamma_A}{\partial t}\right)r\,dr = 2\pi nF\int_0^{r_d}\text{div}\left\{D^{EH}\left[(\text{grad}\,\Gamma_A) - 2\beta\frac{nF}{R_gT}\Gamma_A(\text{grad}\,E^*)\left(1-\frac{\Gamma_A}{\Gamma^0}\right)\right]\right\}r\,dr + 2\pi nF\int_0^{r_d}[-k_f\Gamma_A + k_b(\Gamma^0-\Gamma_A)]r\,dr \quad (29)$$

The last integral on the right-hand side of eq 29 represents the total current exchanged with the metal electrode. It then follows that

$$\int_0^{r_d}\frac{1}{r}\frac{\partial}{\partial r}\left\{rD^{EH}\left[(\text{grad}\,\Gamma_A) - 2\beta\frac{nF}{R_gT}\Gamma_A(\text{grad}\,E^*)\times\left(1-\frac{\Gamma_A}{\Gamma^0}\right)\right]\right\}r\,dr = 0 \quad (30)$$

Integration of the latter equation yields

$$\left\{rD^{EH}\left[(\text{grad}\,\Gamma_A) - 2\beta\frac{nF}{R_gT}\Gamma_A(\text{grad}\,E^*)\left(1-\frac{\Gamma_A}{\Gamma^0}\right)\right]\right\}_{r=r_d} - \left\{rD^{EH}\left[(\text{grad}\,\Gamma_A) - 2\beta\frac{nF}{R_gT}\Gamma_A(\text{grad}\,E^*)\left(1-\frac{\Gamma_A}{\Gamma^0}\right)\right]\right\}_{r=0} = 0 \quad (31)$$

from which it is readily obtained that

$$\left\{D^{EH}\left[(\text{grad}\,\Gamma_A) - 2\beta\frac{nF}{R_gT}\Gamma_A(\text{grad}\,E^*)\left(1-\frac{\Gamma_A}{\Gamma^0}\right)\right]\right\}_{r=r_d} = 0 \quad (32)$$

which is the required boundary condition at the disk electrode edge. Note that if for whatever reason it might be that there is no EH process occurring at the SAM surface, then $D^{EH} = 0$ and the boundary condition in eq 32 would always be fulfilled whatever the distribution of Γ_A and E^*. In fact, in this situation (i.e., when $D^{EH} = 0$) the concentration at the disk edge would be governed by the kinetic rate law

(6) Amatore, C. Principles and Methods. Basic Concepts. In *Organic Electrochemistry*; Lund, H., Hammerich, O., Eds.; Marcel Dekker: New York, 2000; Chapter 1, pp 1−94.
(7) (a) Savéant, J.-M. *J. Electroanal. Chem.* **1986**, *201*, 211. (b) Savéant, J.-M. *J. Electroanal. Chem.* **1987**, *227*, 299. (c) Savéant, J.-M. *J. Phys. Chem.* **1988**, *92*, 4526. (d) Andrieux, C. P.; Savéant, J.-M. *J. Phys. Chem.* **1988**, *92*, 6761. (e) Savéant, J.-M. *J. Electroanal. Chem.* **1988**, *242*, 1.
(8) See, e.g.: Penner, R. M.; Van Dyke, L. S.; Martin, C. R. *J. Phys. Chem.* **1988**, *92*, 5274.

$$\left(\frac{\partial \Gamma_A}{\partial t}\right)_{r_d} = [-k_f \Gamma_A + k_b(\Gamma^0 - \Gamma_A)]_{r_d} \quad (33)$$

which would also apply at any point of the disk electrode surface under such conditions.

In this work, we use Butler−Volmer rate laws for electron transfer kinetics both with the metal electrode and for electron hopping. Indeed, all cases examined here involve small overpotentials in each case. This will be readily apparent in the following for EH. The same occurs for electron transfers with the metallic electrode despite the fact that the voltammetric waves may be rather shifted vs their standard potential with large peak-to-peak separations (ΔE_p). Indeed, the largest contributions to ΔE_p considered here represent an ohmic drop and lagging capacitance charging (compare Figure 2 and see below) rather than the result of extremely small heterogeneous rate constants. Hence, except for unusual systems in which the transfer coefficient would vary drastically with the kinetic overpotential, the two formulations of electron transfer rate constants (viz., Marcus vs Butler−Volmer) result in the same rate law, which is more simply described by the Butler−Volmer one.

Finally, let us mention that, when taking into account the condition in eq 32, the integral of eq 23 over the electrode surface confirms that the overall faradic current flowing through the system corresponds only to electrons exchanged with the metallic electrode:

$$i_f = -2\pi nF \int_0^{r_d} [k_f \Gamma_A - k_b(\Gamma^0 - \Gamma_A)] r \, dr \quad (34)$$

Coupling with Ohmic and Capacitive phenomena. The above section has shown that EH redistribution of charges across the SAM surface critically depends on the gradient of E^* across the system. This is imposed by the delicate interplay between capacitive and faradic currents which has been previously described in a former work of ours,[2] since this was derived within the most general electrochemical background. However, owing to the perfect 2D nature of the SAM system, it is advisable to rewrite eq 12 as in ref 2 in terms of local current densities rather that in terms of local currents.

This follows readily upon dividing all terms in the former equation by the area of the infinitesimal ring $2\pi r \, dr$:

$$vC_{dl}^{sp} - j_{cap}(r,t) = dR_e(r) \, dC_{dl}(r) \left[\frac{\partial j_{cap}(r,t)}{\partial t} + \frac{\partial j_f(r,t)}{\partial t}\right] \quad (35)$$

where C_{dl}^{sp} is the specific capacitance (μF/cm^2) of the electrode/solution interface per unit area and j_{cap} and j_f are the local capacitive and faradic current densities, respectively. As noted above, at each moment the faradic current flowing through one infinitesimal ring at distance r from the system center is given by the time variation of the surface concentration of A at the same moment and same point. It follows that di_f and j_f are

$$\begin{aligned} di_f(r,t) &= nF\left(\frac{\partial \Gamma_A}{\partial t}\right)_r 2\pi r \, dr \\ j_f(r,t) &= nF\left(\frac{\partial \Gamma_A}{\partial t}\right)_r \end{aligned} \quad (36)$$

where $(\partial \Gamma_A/\partial t)_r$ is given by eq 27. This allows reformulating eq 35 as

$$vC_{dl}^{sp} - j_{cap}(r,t) = dR_e(r) \, dC_{dl}(r) \left[\frac{\partial j_{cap}(r,t)}{\partial t} + nF\frac{\partial^2 \Gamma_A}{\partial t^2}\right] \quad (37)$$

In eqs 35 and 37 $dR_e(r) \, dC_{dl}(r)$ is the local time constant.[2] Note again that, though each of its terms is a differential element, $dR_e(r) \, dC_{dl}(r)$ has a finite value because $dC_{dl}(r)$ varies as dr while $dR_e(r)$ depends reciprocally on it:

$$\begin{aligned} dR_e(r) &= \frac{\sqrt{r_d^2 - r^2}}{4\gamma r \, dr} \\ dC_{dl}(r) &= (2\pi r \, dr) C_{dl}^{sp} \\ dR_e(r) \, dC_{dl}(r) &= \frac{\pi}{2} \frac{\sqrt{r_d^2 - r^2}}{\gamma} C_{dl}^{sp} \end{aligned} \quad (38)$$

where γ is the conductivity of the solution. Equations 3 and 37 together with eq 27 and its boundary conditions 28 and 32 define the mathematical framework that governs the three unknowns Γ_A, E^*, and j_{cap}. To finalize the problem, this system of equations must be complemented by the following initial and boundary conditions:

$$t = 0, \quad 0 \le r \le r_d, \quad \Gamma_A = \Gamma^0, \quad E^* = E_{min}, \quad j_{cap} = 0 \quad (39a)$$

$$t > 0, \quad r = 0, \quad \frac{\partial E^*}{\partial r} = 0, \quad \frac{\partial j_{cap}}{\partial r} = 0 \quad (39b)$$

$$t > 0, \quad r = r_d, \quad E^* = E, \quad j_{cap} = vC_{dl}^{sp} \quad (39c)$$

Two of these conditions (39a) and (39b) are obvious. Condition 39a expresses the initial status of the system before the voltammetric scan is performed whenever it is assumed that this starts from a potential where Γ_B is negligible. Equation 39b follows from the symmetry at the disk axis. The third one, viz., eq 39c follows from the fact that $dR_e(r) \, dC_{dl}(r)$ tends to zero when $r \to r_d$ (compare eq 37).[2] Indeed, from eq 3 one obtains immediately that $E^* = E$ at $r = r_d$, and similarly eq 37 affords $j_{cap} = vC_{dl}^{sp}$ at the SAM electrode edge.

FORMULATION OF THE PROBLEM IN DIMENSIONLESS QUANTITIES

For convenience of the numerical simulations and to impart generality to the results that will be presented, it was advisible to recast the above formulation into a set of dimensionless quantities. For this purpose let us introduce the following dimensionless variables for surface concentration (Γ), radial coordinate (R), current density (J), time (τ), heterogeneous rate constant (K_0), EH diffusion (τ_D), potentials (θ and θ^*), and charging time constant (τ_{ch}):

$$\Gamma = \frac{\Gamma_A}{\Gamma^0}, \quad R = \frac{r}{r_d}, \quad J = j\frac{4R_gT}{n^2F^2|v|\Gamma^0}$$
$$\tau = \frac{t}{t_{ch}}, \quad K_0 = t_{ch}k_0, \quad \tau_D = (D^{EH}t_{ch})/{r_d}^2$$
$$\theta = \frac{F}{R_gT}(E - E^0), \quad \theta^* = \frac{F}{R_gT}E^*, \quad \tau_{ch} = \frac{t_{ch}}{dR_e(R)\, dC_{dl}(R)} \tag{40a}$$

In the above, t_{ch} is any suitable time duration that may be selected as a reference for the system and the current densities are normalized to that predicted for a planar SAM electrode at the reversible voltammetric peak.[1] For simplifying the mathematical dimensionless formulation, t_{ch} was selected as the time duration required for achieving an electrokinetic potential change $V_{ch} = F\Gamma^0/C_{dl}^{sp}$ that would correspond to the full charging of the SAM if this was acting as a real capacitance:

$$t_{ch} = \left|\frac{V_{ch}}{v}\right| = \left|\frac{F\Gamma^0}{C_{dl}^{sp}v}\right| \tag{40b}$$

Selecting this reference time implies the introduction of the following auxiliary dimensionless parameters:

$$\theta_{ch} = \frac{F}{R_gT}V_{ch}, \quad \sigma = \frac{Ft_{ch}}{R_gT}v \tag{40c}$$

Note that the absolute values of the latter parameters are the same though their signs may differ owing to the direction of the voltammetric scan. Use of the dimensionless variables and parameters in eqs 40a−40c allows recasting the above physicomathematical model as follows:

$$\frac{\partial\Gamma}{\partial\tau} = -K_f\Gamma + K_b(1 - \Gamma) + \tau_D\left\{\frac{\partial^2\Gamma}{\partial R^2} + \frac{1}{R}\frac{\partial\Gamma}{\partial R} - 2\beta n\left[\Gamma(1 - \Gamma)\left(\frac{\partial^2\theta^*}{\partial R^2} + \frac{1}{R}\frac{\partial\theta^*}{\partial R}\right) + (1 - 2\Gamma)\frac{\partial\Gamma}{\partial R}\frac{\partial\theta^*}{\partial R}\right]\right\} \tag{41a}$$

$$\frac{\partial^2\Gamma}{\partial\tau^2} = -\frac{n\theta_{ch}}{4}\frac{\partial J_{cap}}{\partial\tau} - \frac{n\theta_{ch}\tau_{ch}(R)}{4}J_{cap} + \frac{\mathrm{sign}(\sigma)}{n}\tau_{ch}(R) \tag{41b}$$

$$\theta^* = \theta - \frac{\theta_{ch}}{\tau_{ch}(R)}\left\{\frac{n^2\theta_{ch}}{4}J_{cap} + n\frac{\partial\Gamma}{\partial\tau}\right\} \tag{41c}$$

where the potential dependence of the dimensionless rate constants is given by

$$K_{f,b} = K_0\exp\left[\begin{matrix}-\alpha\\(1 - \alpha)\end{matrix} n\theta^*\right] \tag{42}$$

This set of coupled equations is associated with the following initial and boundary conditions:

$$\tau = 0, \quad 0 \le R \le 1, \quad \Gamma = 1, \quad \theta^* = \theta_{min}, \quad J_{cap} = 0 \tag{43a}$$

$$\tau > 0, \quad R = 0, \quad \frac{\partial\Gamma}{\partial R} = 0, \quad \frac{\partial\theta^*}{\partial R} = 0, \quad \frac{\partial J_{cap}}{\partial R} = 0 \tag{43b}$$

$$\tau > 0, \quad R = 1, \quad \theta^* = \theta, \quad J_{cap} = \mathrm{sign}(\sigma)\frac{4}{n^2\theta_{ch}} \tag{43c}$$

and

$$\tau_D[(\mathrm{grad}\,\Gamma) - 2n\beta\Gamma(1 - \Gamma)(\mathrm{grad}\,\theta^*)]_{R=1} = 0 \tag{44}$$

Note again the following caveat: whenever τ_D is null, the bracket in eq 44 need not be null. For this reason we kept the factor τ_D in the formulation of eq 44 though this is a constant for a given system (i.e., a given simulation).

NUMERICAL SIMULATIONS

Treatment of Second-Order Time Derivatives. Differential eq 41b is of the second order with respect to time. To simplify the numerical treatment of the overall system, we used the standard method for decreasing the order through the artificial introduction of two auxiliary variables defined as

$$\Gamma_1 = \Gamma, \quad \Gamma_2 = \frac{d\Gamma}{d\tau} \tag{45}$$

This amounts to replacing eqs 41b and 41c by the following three equations:

$$\Gamma_2 = \frac{d\Gamma_1}{d\tau} \tag{46a}$$

$$\frac{d\Gamma_2}{d\tau} = -\frac{n\theta_{ch}}{4}\frac{dJ_{cap}}{d\tau} - \frac{n\theta_{ch}\tau_{ch}}{4}J_{cap} + \frac{\mathrm{sign}(\sigma)}{n}\tau_{ch} \tag{46b}$$

$$\theta^* = \theta - \frac{\theta_{ch}}{\tau_{ch}}\left\{\frac{n^2\theta_{ch}}{4}J_{cap} + n\Gamma_2\right\} \tag{46c}$$

For the auxiliary variable Γ_1 this set of equations is associated with the same boundary conditions given above for Γ though after permutation of Γ into Γ_1; see eqs 43a, 43b, and 44. For Γ_2, since eq 46a is fulfilled at any time and any location, it can be used at the SAM edge and center as well. The initial condition $\Gamma_2(\tau = 0) = 0$ was used for this unknown provided that the starting potential value was sufficiently far from the formal potential E^0 of the redox couple. Finally, for θ^* eqs 43a−43c still apply since they are not affected by the change of its definition from eq 41c to eq 46c.

Coordinate Transformation and Numerical Solution. Numerical simulation of the system at hand faces severe difficulties due to several factors. First, eqs 41a and 46a−46c form a strongly nonlinear system of differential-algebraic equations owing to the products of concentration- and potential-dependent terms in eq 41a and exponential dependence of normalized rate constants K_f and K_b on the effective overpotential θ^*. The second issue is related to the fact that under most interesting conditions from the experimental point of view (fast voltammetric scans and

fast ET reactions) all the quantities Γ, θ^*, and J_{cap} experience extremely rapid variations in the vicinity of the disk edge, leading to very high spatial gradients and time derivatives of these quantities (see below). Moreover, eqs 41a and 46a−46c are not well-conditioned (viz., their finite-difference approximations may be sensitive to possible numerical errors), which, together with rapid changes of dependent variables, may lead to nonphysical solutions or oscillations in the numerical solution. Therefore, the numerical procedure for the solution of this problem needed to be carefully constructed by taking into account all the above issues.

To enhance the approximation of steep gradients of Γ, θ^*, and J_{cap} in the vicinity of the disk edge, we resorted to a transformation of the radial coordinate derived from the conformal mapping previously developed by some of us[9] for the solution of diffusional mass transport from the solution toward an embedded disk electrode. This amounts to the following change of variable in the governing equations along the segment $Z = 0$, $0 \le R \le 1$:

$$R = \sin\left(\frac{\pi}{2}\xi\right) \tag{47}$$

Although extremely efficient in this work for the range of parameters investigated, it is noted that on a formal basis this transformation cannot always be considered as the most adequate one. Though it is perfectly suited for any pure 3D diffusion reaction problem occurring at a disk electrode, the system under scrutiny is much more complex due to the presence of mathematical difficulties in eq 27. Therefore, a higher compression of space near the disk electrode edge may be required whenever the parameters which determine the gradients reach extremely high (though experimentally unrealistic) values.

Upon introducing this coordinate transformation, the terms of eq 41a containing spatial differentials acquired nonconstant coefficients which we do not detail here since they can be readily obtained from the differentiation of eq 47.

The resulting equations were discretized in the conformal space using the fully implicit method. To ensure the stability of the simulation procedure, special care was taken in using approximations of the same order of accuracy for all equations in the system. This was particularly crucial for the approximation of boundary condition 44 at the disk edge since it depends on highly variable gradients of concentration and overpotential (see below). To construct a good approximation, eq 41a was integrated over the area of the last grid element located between $R = 1 - \Delta R$ and $R = 1$, where ΔR is the size of the last grid step. This yielded

$$2\pi\Delta R\left(\frac{\partial\Gamma}{\partial\tau}\right)_{R=1} = 2\pi\tau_D[\text{grad}\,\Gamma - 2\beta n\Gamma(1-\Gamma)(\text{grad}\,\theta^*)]_{R=1} - 2\pi(1-\Delta R)\tau_D[\text{grad}\,\Gamma - 2\beta n\Gamma(1-\Gamma)(\text{grad}\,\theta^*)]_{R=1-\Delta R} + 2\pi\Delta R[-K_f\Gamma + K_b(1-\Gamma)]_{R=1} \tag{48}$$

According to the boundary condition in eq 44, the first term on the right-hand side of 48 is exactly zero. Hence, the numerical approximation at the boundary takes the form

$$\left(\frac{\partial\Gamma}{\partial\tau}\right)_{R=1} + \tau_D\frac{1-\Delta R}{\Delta R}[\text{grad}\,\Gamma - 2\beta n\Gamma(1-\Gamma)(\text{grad}\,\theta^*)]_{R=1-\Delta R} + [K_f\Gamma - K_b(1-\Gamma)]_{R=1} = 0 \tag{49}$$

where the time derivative and gradients were then approximated using finite differences as usual. It should be noted that this approximation is second-order accurate in ΔR and thus is consistent with the approximation of spatial derivatives in eq 41a for $R < 1$. The use of the coordinate transformation in eq 47 and the boundary condition approximation in eq 49 (note that it is formulated in terms of the normalized coordinate R for clarity) allowed stable results without nonphysical oscillations to be obtained.

The discrete equivalents of eqs 41a and 46a−46c with the corresponding initial and boundary conditions in eqs 43a−43c and 44 were solved using a modified Newton method for nonlinear algebraic systems. Numerical experiments established that a grid of size $NR \times N\tau = 2000 \times 2000$ was sufficient for achieving an accuracy better than 0.01% for all the results quoted here.

A computer program performing the numerical solution of the problem at hand was written in Borland Delphi 7 Enterprise Edition and executed on a PC equipped with an Intel Pentium 4 processor at 3 GHz and 512 MB of RAM with typical run times of less than 80 s. This specific program will be integrated in new software, KISSA, presently under development, for treating any electrochemical mechanism including ohmic and capacitive distortions following our theoretical works on this subject.[2,3]

RESULTS

The present model was solved upon considering or not ($D^{EH} = 0$) the effect of electron hopping on the voltammetric behavior of SAMs. In both cases, the contributions of an ohmic drop and capacitive time constant were found identical to those previously described and discussed for the case of very thin layer films deposited at disk microelectrodes.[3] This result was expected since when a very thin layer film is involved the electrochemical situation in terms of an ohmic drop and capacitive currents is necessarily similar to that for a SAM since both feature essentially 3D ionic transport into the electrolyte, the SAM or the thin layer film only acting as a 2D boundary condition in this respect. For these reasons, these effects will not be described or discussed again, and the reader is referred to our previous paper.[3]

We will therefore focus hereafter on the matters which are concerned with electron hopping. Indeed, generally experimentalists do not consider this possibility in rationalizing SAM voltammetry. However, the strong gradients of potential created near the edge of the electrode, as we already reported and discussed for thin layer films,[3] may be thought to generate specific voltammetric features due to the importance of such terms in eq 27. One goal of the following is then to examine whether this issue may lead to significant errors in the interpretation of SAM voltammetry under conditions of high ohmic drop effects.

Figure 3 reveals overall voltammetric currents (blue curves) together with their faradic (red curves) and capacitive (green curves) components computed for typical values of physicochemical parameters for a series of increasing voltammetric scan rates. The value of the hopping diffusion coefficient $D^{EH} = 5 \times 10^{-6}$ $cm^2\ s^{-1}$ was taken from the literature and corresponds to

(9) Amatore, C.; Oleinick, A.; Svir, I. *Electrochem. Commun.* **2004**, *6*, 588–594.

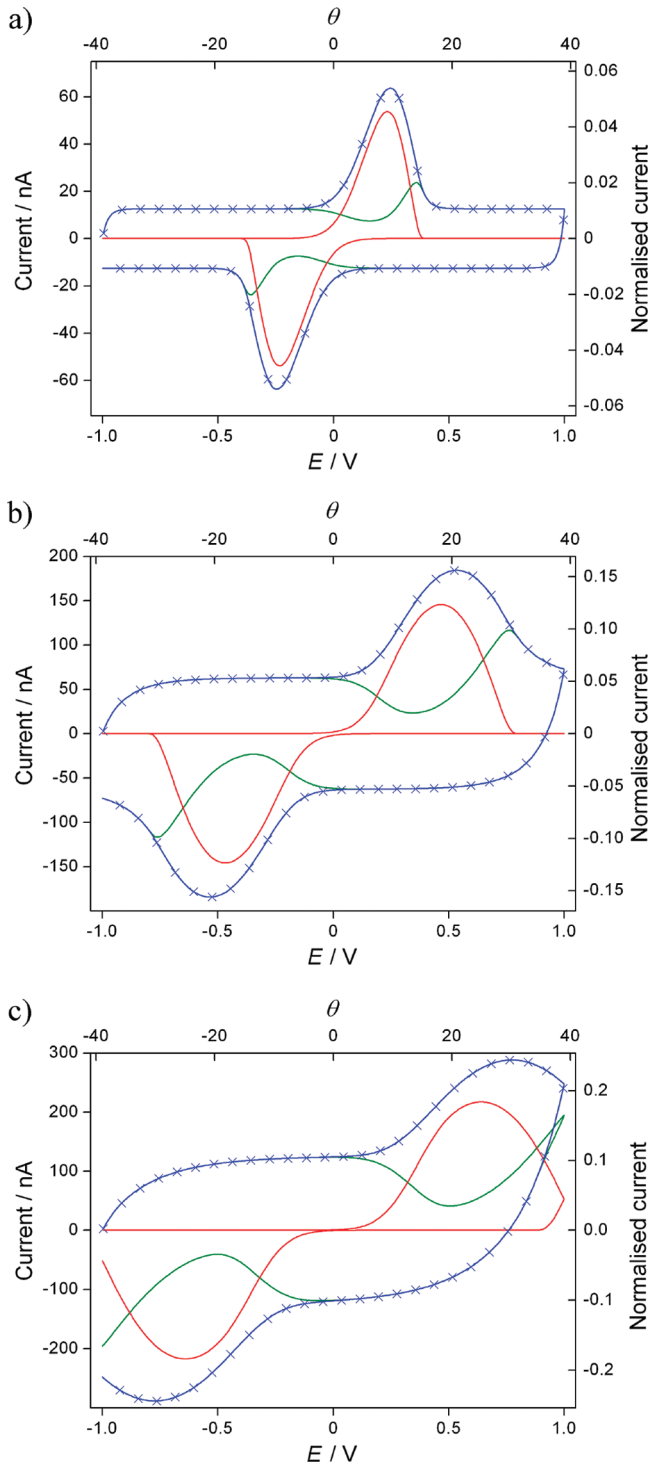

Figure 3. Simulated voltammograms for dimensionless parameters $\theta_{ch} = |\sigma| = 37.59$, $K_0 = 9.65 \times 10^{-2}$, and $\tau_D = 1.21 \times 10^{-3}$ that correspond, for instance, to the following dimensioned ones: $r_d = 2\mu m$, $\Gamma_0 = 1 \times 10^{-10}$ mol cm^{-2}, $D^{EH} = 5 \times 10^{-6}$ cm^2 s^{-1}, $n = -1$ (oxidation), $k_0 = 1 \times 10^4$ s^{-1}, $E^0 = 0$, $C_{dl}^{sp} = 1 \times 10^{-5}$ F cm^{-2}, $\gamma = 1 \times 10^{-3}$ A V^{-1} cm^{-1}, $\alpha = \beta = 0.5$, $E_{min} = -1$ V, $E_{max} = 1$ V. (a) $v = 1 \times 10^4$ V s^{-1} ($\tau_{ch}(0) = 30.71$); (b) $v = 5 \times 10^4$ V s^{-1} ($\tau_{ch}(0) = 6.14$); (c) $v = 1 \times 10^5$ V s^{-1} ($\tau_{ch}(0) = 3.07$). The symbols indicate simulations without electron hopping ($D^{EH} = 0$).

relatively fast electron hopping; i.e., it is supposed to involve adjacent redox centers with an already very high rate constant of exchange.[10] Nevertheless, the simulation results show that there is virtually no dependence of voltammetric shapes on

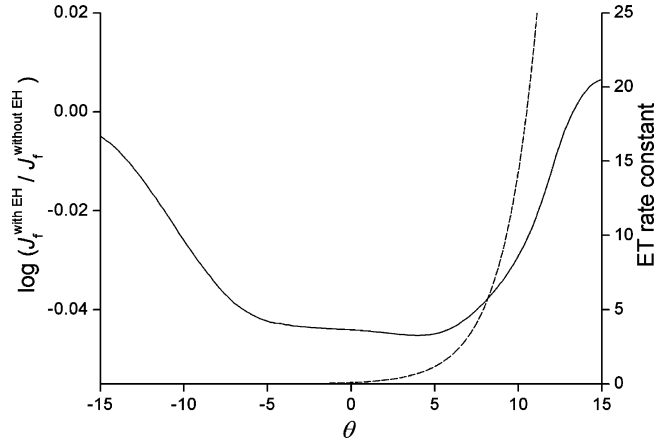

Figure 4. Comparison between simulated dimensionless faradic currents with and without EH (solid curve) and the dimensionless kinetic rate constant (dashed curve). Parameters are the same as for Figure 3c.

hopping diffusion. This is confirmed by the superimposition of voltammograms computed for $D^{EH} = 0$ shown with symbols in Figure 3.

A closer examination evidences a slight discrepancy between voltammograms simulated with and without hopping diffusion near the foot of the voltammetric wave, i.e., when the faradic current begins to rise. Figure 4 illustrates the variations of the ratio of faradic currents computed with and without EH over the potential range corresponding to the onset of electron transfer kinetics between the SAM and the electrode. These conditions correspond to the largest impact of the hopping diffusion for the situations envisioned here. It is over this range that the concentration and potential gradients attain their largest values at the electrode edge, thus enforcing the strongest lateral EH transport. Even so, in this area the value $\log(J_f^{with\ EH}/J_f^{without\ EH})$ differs only slightly from zero (Figure 4). At larger times the gradients of concentration, effective overpotential, and current densities gradually relax, leading to the disappearance of any diffusion effect on the overall current. The same occurs for the backward wave near the foot of the faradic reduction wave.

To understand this behavior, one must consider the relative contributions of hopping diffusion and kinetic terms in eq 41a. Indeed, the impact of EH on the current density due to the lateral redistribution of charges is governed by the magnitude of the following ratio:

$$\left|\frac{\mathrm{div}\, J^{EH}}{J^{ET}}\right| \propto \frac{\tau_D}{K_0} e^{\alpha n \theta^*} \qquad (50)$$

where $J^{ET} = -K_f\Gamma + K_b(1 - \Gamma)$. This ratio compares the electron hopping contribution to that of the exponentially increasing rate constant of the direct electron transfer with the metal electrode. The cause of the restriction of the importance of EH-related effects to a rather narrow zone near the voltammetric wave foot is readily apparent from eq 50. Indeed, this shows that the right-hand side of eq 50 may be large only for sufficiently small (or even negative) overpotentials. However, by

(10) (a) Amatore, C.; Bouret, Y.; Maisonhaute, E.; Goldsmith, J. I.; Abruña, H. D. *ChemPhysChem* **2001**, *2*, 130–134. (b) Amatore, C.; Bouret, Y.; Maisonhaute, E.; Goldsmith, J. I.; Abruña, H. D. *Chem.—Eur. J.* **2001**, *7*, 2206–2226.

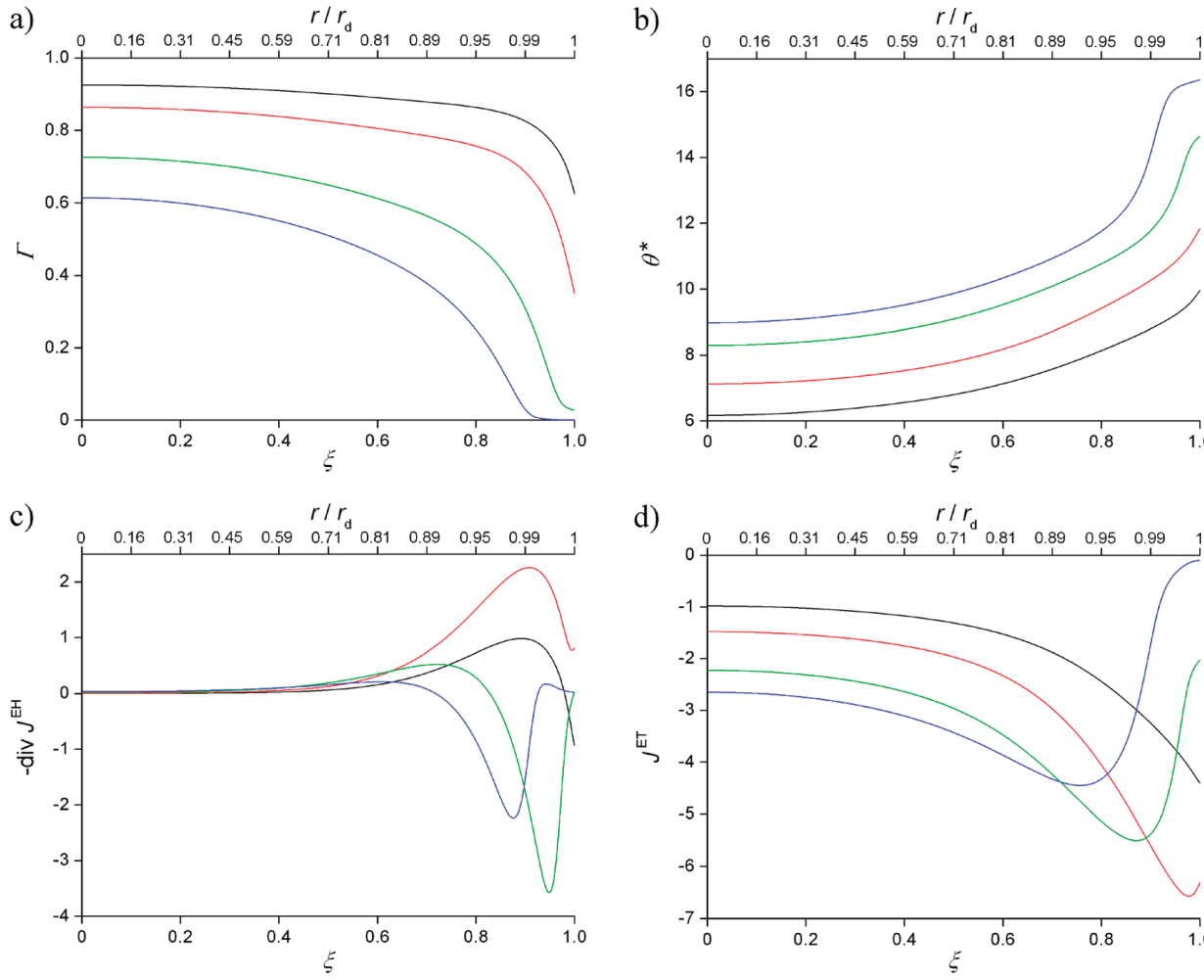

Figure 5. Development of the main normalized quantities in the range of the dominant EH effect ($\tau_D/K_0 = 1.25$): (a) concentration; (b) overpotential; (c) divergence of the EH flux; (d) ET flux. The curves correspond to $\Delta\theta = \theta_p - \theta = 7.79$ (black), $\Delta\theta = 5.92$ (red), $\Delta\theta = 3.12$ (green), and $\Delta\theta = 1.40$ (blue). See the text for other parameter values. Note that the different curves are presented in the conformal space coordinate (ξ). The upper horizontal scale (i.e., the real space coordinate) shows that the sharpest features occur in a narrow region near the electrode edge.

definition, under such conditions there is no significant electron transfer between the active centers of adsorbed molecules and the electrode. Thus, concentration gradients within the SAM are virtually zero, and the same is true for the gradient of θ^*. Therefore, the EH effect is then necessarily small. It will then always be restricted to the foot of the faradic wave unless τ_D/K_0 is excessively large compared to its experimentally realistic range. As the overpotential increases, the ET rate constant grows exponentially and thus quickly outpaces electron hopping diffusion unless the gradients in eq 27 become infinite though this may occur only at the very edge of the disk electrode and provided that τ_D/K_0 is large enough as will be shown below. Figure 4 thus only confirms that the effect of EH is not negligible only in a narrow potential zone where the concentration Γ is sharply depleted and θ^* also varies suddenly near the electrode edge. This creates an EH wave propagating toward the electrode center, yet as will be shown below, even in extreme (and experimentally unrealistic) cases this wave is rapidly smoothed after traveling a short distance from the electrode edge. Hence, the overall effect becomes negligible.

To achieve a more tangible influence of EH diffusion on the voltammetry, one has to either consider unrealistically high diffusion rates (e.g., 2 or 4 orders of magnitude higher than the fastest ones reported in the literature) or assume the disk radius to be in the range of a few tens of nanometers. The former is not a physically realistic case since this would involve hopping rate constants beyond the maximum kinetic limit while in the latter case the system would no longer follow the statistical laws derived here[11] in the range where the EH wave is significant (see below). However, computations may be performed under such unrealistic conditions to evidence the distributions of the concentration, effective overpotential, and current densities that are expected under situations where EH would have a more significant effect.

Figure 5 evidences the variations across one electrode radius for each relevant quantity over the potential range before the voltammetric peak and corresponds to $K_0 = 4.82 \times 10^{-2}$, $\tau_D = 6.03 \times 10^{-2}$, $\tau_{ch}(0) = 15.36$, and $\theta_{ch} = |\sigma| = 37.59$. Curves of the same color correspond to the same value of the potential such as $\theta = \theta_p - \Delta\theta$, where θ_p is the voltammetric peak potential under these conditions. One can observe that EH and ET fluxes undergo sudden shape transitions over this potential range in agreement with the observation in Figure 4. However,

(11) Amatore, C.; Grün, F.; Maisonhaute, E. *Angew. Chem.* **2003**, *42*, 4944–4947.

Figure 5 establishes that these variations are restricted to an extremely narrow area near the electrode edge. These strong and sudden changes are readily smoothed when the corresponding EH wave propagates toward the electrode center. Note that the distributions in Figure 5 are plotted versus the conformal coordinate ξ, which is greatly expanded near the electrode edge; compare these to the upper horizontal axes that show the values of the normalized radius. Thus, most of the EH wave is attenuated within 1% of the disk radius. This is a negligibly small area. Even for micrometric electrodes it corresponds to an area where the SAM is expected to be poorly defined anyway. Therefore, it is presumed that such an effect will not be observable experimentally.

The results presented in Figure 5 correspond to the parameter values given in Figure 3 with, for instance, the following exceptions: $D^{EH} = 5 \times 10^{-4}$ cm^2 s^{-1}, $\gamma = 1 \times 10^{-2}$ A V^{-1} cm^{-1}, and $v = 2 \times 10^5$ V s^{-1}. Such values of D^{EH} and γ are extremely high and clearly unrealistic for real SAM systems. Alternatively, the same set of dimensionless parameters may feature a nanoelectrode with $r_d = 200$ nm, $v = 2 \times 10^5$ V s^{-1}, and other parameters having realistic values (see the caption of Figure 3). In this case the delicate effects appearing at the extreme edge of the electrode, as shown in Figure 5, would not be experimentally realistic due to (i) the molecular size being non-negligible versus the dimension of the electrode zone (ca. 2 nm!) where they take place and (ii) inevitable imperfections of the electrode shape and SAM ordering which would alter the distributions of all quantities in this area.

The above discussion shows that under realistic experimental conditions the electron hopping diffusion should not reveal itself on voltammetric waves. This validates the usual practice of neglecting EH effects though this analysis shows that, in the absence of ohmic drop online compensation,[4] proper rationalization of voltammetric data requires considering the microscopic resistive and capacitive effects.

CONCLUSIONS

This work completes a series of papers in which the distortions introduced by solution resistance in voltammetric waves have been carefully analyzed for the case of disk electrodes and single electron transfer mechanisms. As established in previous work for classical electrochemistry in 3D electroactive solutions, or for very thin electroactive layers, we confirmed here that an uncompensated ohmic drop significantly alters voltammetry waves even at microelectrodes. This occurs in two ways. One results directly from the dependence of the ohmic drop across the electrode radius due to locally varying resistance and varying current density. The other features the ensuing distortions incurred in the faradically effective potential due to the variations of time constants across the microelectrode. In other words, not all the electrode surface experiences the same charging time duration.

For SAMs these effects were found to be very similar to those discussed previously for very thin redox films.[3] This is not a surprising conclusion since in both cases the redox-active area acts as a 2D (SAM) or near-2D (thin film) boundary condition while ohmic drop losses are regulated by ionic transport within the surrounding electrolyte over distances that exceed those of the electrode, hence of any thin film or SAM.

In addition to our previous work on thin redox films, we investigated here whether gradients of faradically active potentials across the electrode surface could stimulate electron hopping across the SAM so as to rehomogenize the gradients generated by ohmic and capacitive distortions. For this purpose a new and general theory of electron hopping under conditions of diffusion−migration has been derived rigorously. This is by no means restricted to the present case and may be readily adapted to other circumstances including 3D-developed redox systems with immobile centers thanks to the generality of its formulation.

This precise analysis of electron hopping established that, under any realistic circumstances, EH contributions may not significantly compensate ohmic and capacitive alterations over the whole voltammogram. Overall, these contributions are minimal to voltammetric waves for realistic systems, though they significantly change local concentration and potential distributions near the disk electrode edge. However, these changes are readily dissipated while the EH perturbation propagates away from the microelectrode edge. This validates a posteriori the usual neglecting of this effect in analyzing SAM voltammetric data even when these are severely affected by ohmic and capacitive components which need to be accounted for as discussed in this work.

ACKNOWLEDGMENT

This work was partially supported by the CNRS (UMR 8640 "PASTEUR"), Ecole Normale Superieure (ENS), University Pierre and Marie Curie (UPMC), and French Ministry of Research. We thank the Ministry of Education and Science of Ukraine and the French Ministry of Foreign Affairs (EGIDE) for a "DNIPRO" research grant. I.S. thanks Mairie de la Ville de Paris for a senior scientist research grant.

APPENDIX

Latin Symbols

A, B − electroactive species

C_{dl}^{sp} − specific capacitance of the electrode/solution interface (F cm^{-2})

D^{EH} − diffusion coefficient of electron hopping (cm^2 s^{-1})

$dC_{dl}(r)$ − capacitance of an elementary ring on the disk surface (F)

$di(r)$ − overall (capacitive + faradic) current of an elementary ring on the disk surface (A)

di_f − elementary faradic current (A)

dN_A − elementary amount of A (mol)

dr − thickness of an infinitesimal concentric ring on the disk electrode surface (cm)

$dR_e(r)$ − uncompensated resistance of an elementary ring on the disk surface (Ω)

dt − elementary time interval (s)

$dW^{\pm}$ − energetic change associated with EH (J)

E − applied potential (V)

EH − electron hopping

E^0 − formal potential of the A/B redox couple (V)

E_{in} − initial potential of the voltammetric scan (V)

E_{min}, E_{max} − minimum and maximum potentials during voltammetric scan (V)

E_{SAM} − effective potential experienced by the SAM molecules (V)

E^* − local overpotential effecting electron transfer (ET) between the SAM and the electrode (V)

F — Faraday constant (F mol^{-1})
i^{EH} — overall current due to electron hopping (A)
i_f — overall faradic current (A)
j_{cap}, j_f — local capacitive and faradic current densities (A cm^{-2})
J_{cap} — dimensionless capacitive current density
$J^{EH}_{A,r}(r)$ — apparent radial flux of A due to electron hopping (mol cm^{-1} s^{-1})
n — number of transferred electrons
k^+, k^- — bimolecular EH rate constants (mol^{-1} cm^2 s^{-1})
k_0 — standard electrochemical rate constant of ET between the SAM and the electrode (s^{-1})
K_0 — dimensionless ET rate constant
k_f, k_b — rate constants of ET between the SAM and the electrode (s^{-1})
K_f, K_b — normalized ET rate constants
k_0^{EH} — intrinsic electron hopping rate constant (mol^{-1} cm^2 s^{-1})
r — distance from the electrode center (radial coordinate, cm)
R — normalized radial coordinate
r_d — disk electrode radius (cm)
R_g — universal gas constant (J mol^{-1} K^{-1})
t — time (s)
t_{ch} — reference time duration (s)
T — temperature (K)
v — voltammetric scan rate (V s^{-1})
V_{ch} — reference potential value (V)
z — charge of A

Greek Symbols
α — transfer coefficient of ET between the SAM and the electrode
β — transfer coefficient of electron hopping
γ — solution conductivity (Ω^{-1} cm^{-1})
Γ — normalized concentration of A
Γ^0 — overall surface concentration of the electroactive species (mol cm^{-2})
Γ_1, Γ_2 — auxiliary variables
Γ_A, Γ_B — surface concentrations of electroactive species A and B (mol cm^{-2})
Δ — Laplace operator
μ_m — electrochemical potential of species m (kJ mol^{-1})
μ_m^0 — standard electrochemical potential of species m (kJ mol^{-1})
θ — dimensionless applied potential
θ_{ch} — auxiliary dimensionless parameter
θ_p — dimensionless voltammetric peak potential
θ^* — dimensionless effective overpotential
σ — auxiliary dimensionless parameter
τ — dimensionless time
τ_{ch} — dimensionless charging time constant
τ_D — dimensionless EH diffusion coefficient
ξ — conformal coordinate

Received for review July 8, 2009. Accepted August 29, 2009.

AC901513X